Spatially explicit modeling of PAR transmission and growth of *Picea glauca* and *Abies balsamea* in the boreal forests of Alberta and Quebec

Kenneth J. Stadt, Victor J. Lieffers, Ronald J. Hall, and Christian Messier

Abstract: To investigate the feasibility of a spatially explicit, radiation-based regeneration model for the boreal forest, we tested the predictions of a three-dimensional simulator of photosynthetically active radiation transmission (%PAR), MIXLIGHT, and the growth response of understory *Abies balsamea* (L.) Mill. (balsam fir) and *Picea glauca* (Moench) Voss (white spruce) to %PAR in two large (>1 ha) mixed-species forest sites, one in eastern Canada at Lac Duparquet, Quebec, and one in western Canada at Calling Lake, Alberta. Overstory tree locations and dimensions were obtained from aerial photographs or ground measurements and allometric relationships. Seasonal %PAR calculated by MIXLIGHT for the Calling Lake site was very similar to seasonal %PAR measured by quantum sensors ($n = 5$, %PAR range = 15%–33%, $r = 0.93$). Daily measurements of %PAR were also predicted well by simulations at both sites ($n = 34$–36, %PAR range = 1%–45%, $r \geq 0.76$). Functional relationships, designed to saturate at the maximum height growth potential of these sites, were developed to predict sapling height growth from simulated seasonal %PAR and initial height ($R^2 \geq 0.74$). These results demonstrate the potential of the MIXLIGHT simulator for estimating PAR at microsites within heterogeneous forests and for modeling understory tree growth.

Résumé : De façon à évaluer s'il est possible d'utiliser un modèle spatialement explicite de régénération basé sur le rayonnement en forêt boréale, les auteurs ont testé les prédictions d'un simulateur tridimensionnel de la transmission du rayonnement photosynthétiquement actif (%RPA), MIXLIGHT, et la réponse de croissance d'*Abies balsamea* (L.) Mill. (sapin baumier) et de *Picea glauca* (Moench) Voss (épinette blanche) au %RPA dans deux grands sites (>1 ha) de forêt mélangée, situés l'un au lac Duparquet (Québec) dans l'est canadien et l'autre à Calling Lake (Alberta) dans l'ouest canadien. La localisation et la dimension des arbres du couvert ont été obtenues à l'aide de photographies aériennes, de mesures de terrain et de relations allométriques. La valeur saisonnière du %RPA estimée par MIXLIGHT pour le site de Calling Lake était très proche des valeurs saisonnières du %RPA mesurées à l'aide de quantomètres ($n = 5$, amplitude %RPA = 15 % – 33 %, $r = 0,93$). Des mesures journalières du *%RPA* ont également été bien prédites dans les deux sites par les simulations ($n = 34$–36, amplitude %RPA = 1 % – 45 %, $r \geq 0,76$). Des relations fonctionnelles, conçues pour s'ajuster au potentiel maximal de croissance en hauteur de ces sites, ont été développées pour prédire la croissance en hauteur de jeunes tiges à partir de valeurs saisonnières simulées du %RPA et de la hauteur initiale ($R^2 \geq 0,74$). Ces résultats démontrent que MIXLIGHT peut simuler le RPA dans des microsites au sein de forêts hétérogènes et modéliser la croissance des arbres du sous-bois.

[Traduit par la Rédaction]

Introduction

The complexity of mixed-species forest dynamics, coupled with interest in partial-cut silvicultural systems for managing these forests, has stimulated the development of spatially explicit, process-driven models of forest regeneration (Pacala et al. 1993; Bartelink 2000). These models grow trees according to the local availability of resources, which depends on the spatial configuration, size, and attributes of the trees' neighbours. Photosynthetically active radiation (PAR: 400–700 nm) is typically the resource modeled, as there is consistent evidence that this is the critical resource in many forest types (e.g., Lieffers and Stadt 1994; Pacala et al. 1994; Wright et al. 1998).

PAR availability can be modeled by representing the overlying vegetation at a number of scales, from the entire canopy (Pierce and Running 1988; Black et al. 1991) to small

K.J. Stadt.[1] Department of Renewable Resources, General Services Building 751, University of Alberta, Edmonton, AB T6G 2H1, Canada.
V.J. Lieffers. Department of Renewable Resources, Earth Science Building 442, University of Alberta, Edmonton, AB T6G 2E3, Canada.
R.J. Hall. Canadian Forest Service, Northern Forestry Centre, 5320-122nd Street, Edmonton, AB T6H 3S5, Canada.
C. Messier. Département des sciences biologiques, Université du Québec à Montréal, C.P. 8888, succursale Centre-ville, Montréal, QC H3C 3P8, Canada.

[1]Corresponding author (e-mail: ken.stadt@ualberta.ca).

doi: 10.1139/X04-141

subvolumes of the canopy (Comeau et al. 1998), individual tree crowns (Canham et al. 1994; Cescatti 1997; Brunner 1998; Bartelink 2000; Stadt and Lieffers 2000; Groot 2004), shoots (Perttunen et al. 1998), or even single leaves (Myneni and Impens 1985). The data requirements and computation time increase significantly with the fineness of the scale. However, the canopy scale misses the finer scale spatial variability in PAR created by patch, strip and variable-retention harvests, or found beneath natural mixtures of species with opaque crowns (e.g., *Picea*, *Abies*) among open-crowned species (*Populus*, *Pinus*) in the mixedwood region of the boreal forest (Stadt et al. 1997). The subvolume or tree crown scale is therefore better suited for modeling regeneration in these forests.

Two approaches have been used to relate PAR availability to tree growth. In agricultural crops, biomass increment per unit area is a constant proportion of the energy intercepted in the PAR region (Monteith 1972). This relationship appears to hold for forest stands as well (Grace et al. 1987). The relationship between volume, radial and height growth, and absorbed PAR (APAR) at the individual tree level is also strong, but may be nonlinear (Brunner and Nigh 2000; MacFarlane et al. 2002). Since the determination of APAR is computationally intense, an alternate approach is to relate radial and height growth to the seasonal transmission of above-canopy PAR (%PAR) available to each tree (Pacala et al. 1994; Wright et al. 1998). There is ample evidence that radial and height growth are correlated with %PAR (Lieffers and Stadt 1994; Pacala et al. 1994; Wright et al. 1998; Duchesneau et al. 2001; Claveau et al. 2002). However, the size of the crown should also be an important predictor, since this provides the radiation-absorbing surface. Because of its computational simplicity, we adopted the growth versus %PAR approach.

In earlier work, we described the calibration and stand-scale validation of PAR transmission models for overstory (Stadt and Lieffers 2000) and understory vegetation in western Canadian boreal forests (Stadt 2002). The present study tests the ability of these models, contained in the MIXLIGHT software package, to predict microsite (approx. 1 m^2) variations in PAR transmission and investigates how effectively simulated %PAR can be used to predict the growth of understory trees in boreal forest stands from both western and eastern Canada.

Materials and methods

Site information and mapping

The MIXLIGHT %PAR model was tested in a 1.2-ha (100 m × 120 m) stand in west-central Quebec and a 2.3-ha (102 m × 225 m) stand in north-central Alberta. Stands of these dimensions are necessary to minimize the interception of light from unmapped trees, which can be substantial because of low solar angles at these high latitudes.

The Quebec site was on the west shore of Lac Duparquet on clay soil. The stand was 130 years old, dominated by trembling aspen (*Populus tremuloides* Michx.), with paper birch (*Betula papyrifera* Marsh.), white spruce (*Picea glauca* (Moench) Voss), balsam fir (*Abies balsamea* (L.) Mill.), black spruce (*Picea mariana* (Mill.) B.S.P.), eastern

white cedar (*Thuja occidentalis* L.), and jack pine (*Pinus banksiana* Lamb.) in the overstory (detailed location, climatic, and composition information is given in Table 1). The understory had dense mountain maple (*Acer spicatum* Lam.) and some hazel (*Corylus cornuta* Marsh.) of up to 95% total cover above some microsites. Understory balsam fir were abundant throughout the stand. The site was mapped in 1996 with reference to surveyed 10 m × 10 m grid stakes. Stems of all tree species >5 cm diameter at breast height (1.3 m; DBH) had been measured for DBH and plotted by the bearing and distance from the stem to the nearest stake (C. Kelly and I. Ritchie, personal communication).

The Alberta site was in the central mixedwood natural region 20 km east of Calling Lake, Alberta, on glacial till. The north end of the plot was approximately 80 years old and dominated by trembling aspen, while the south end was 140 years old and dominated by white spruce. A heterogeneous region of mixed spruce and aspen occurred in the centre of the plot. The understory vegetation was a sparse mixture of prickly rose (*Rosa acicularis* Lindl.), marsh-reed grass (*Calamagrostis canadensis* L.), and other shrubs and herbs (up to 35% total cover). Understory white spruce occurred throughout the stand.

The Calling Lake site was stem mapped from large-scale (1:1200) aerial photographs. Photos were acquired 30 March 1999 with a helicopter-mounted aerial camera system (Spencer and Hall 1988). The photos were scanned, aero-triangulated with edge and ground control, and paired into digital stereo models by Integrated Mapping Technologies (Vancouver, British Columbia). To aid in ground control and mapping, a 40 m × 40 m grid of ground control stakes with highly visible targets was surveyed prior to photography.

Crown measurement and mapping was undertaken with a 3-dimensional digital video system (International Systemap Corp., Vancouver, British Columbia). This system measures elevations as well as horizontal coordinates, using stereo parallax and the computer's cursor as the floating dot. We measured the easting, northing, and elevation (i.e., x, y, z) coordinates of the top of each tree's crown and the base of the stem. Tree height was estimated as the difference in the elevation coordinates. To estimate crown radius, we chose two points on opposite sides of the crown at its widest elevation and projected a horizontal circle around the crown, passing through these points. Each tree measurement included the species, the tree height, crown radius, and coordinates of the crown apex.

A ground survey of 68 trees (44 aspen, 24 white spruce) from a range of height and crown radius was performed to check the photo measurements. Correlation coefficients between photo and ground measurements were low for deciduous tree height ($r = 0.59$) because of a lack of contrast between the grey branches and snow-covered ground. However, for deciduous crown radius, conifer height, and crown radius, correlations were considerably better (0.84, 0.97, and 0.93, respectively). Root mean square errors for regressions of photo measurement on ground measurement for deciduous height, deciduous crown radius, conifer height, and conifer crown radius were 2.4, 0.3, 1.6, and 0.2 m, respectively. There was no significant difference between photo and ground measurements for any dimension ($p > 0.415$).

Table 1. Characteristics of the mixed-species boreal sites used to validate the microsite site predictions of the MIXLIGHT %PAR model. Means and range (min–max) are shown for diameter at breast height (DBH).

Characteristic	Lac Duparquet, Quebec	Calling Lake, Alberta*
Site location (latitude and longitude)	48°30′N, 79°20′W	55°30′N, 113°40′W
Ecosite	MS23[†]	BMe[‡]
Slope (%)	12%	Flat
Aspect (°)	110°	
Mean annual temperature[§] (°C)		
Climate normal (1971–2000)	0.7	0.9
During this study (1996–2000)	1.4	2.0
Annual precipitation[‖] (mm)		
Climate normal (1971–2000)	890	454
During this study (1996–2000)	962	397
Stand age (years)	130	80, 140
Top height[¶] (m)	24.4	25.5, 26.0
Density (stems/ha)	3157	579, 1227
Total BA (m^2/ha)	42.0	24.7, 37.1
Aspen BA (m^2/ha)	16.6	22.9, 12.7
Balsam poplar BA (m^2/ha)	0	0, 2.4
Paper birch BA (m^2/ha)	9.8	0, 0.1
White spruce BA (m^2/ha)	8.0	1.7, 21.9
Black spruce BA (m^2/ha)	1.8	0, 0
Balsam fir BA (m^2/ha)	5.8	0, 0
Aspen DBH (cm)	17.7 (1.6–47.1)	22.0 (0.2–90.2)
Balsam poplar DBH (cm)	—	18.1 (1.3–42.4)
Paper birch DBH (cm)	6.8 (0.6–35.9)	8.3 (3.0–16.3)
White spruce DBH (cm)	12.0 (0.6–40.7)	15.8 (0.4–53.1)
Black spruce DBH (cm)	13.5 (0.8–29.9)	—
Balsam fir DBH (cm)	9.1 (0.3–27.3)	—

  *Site spans two stand types: stand age, top height, and basal area at breast height (1.3 m; BA) data are given for aspen-dominated stand, white spruce-dominated stand; size and cover data are summarized for the entire plot.

  [†]Grondin et al. 2000.

  [‡]Beckingham and Archibald 1996.

  [§]Environment Canada 2004.

  [¶]Top height based on the average of the largest diameter 100 trees/ha in the stand.

Relationships among tree and crown dimensions

The full set of crown dimensions for every tree is seldom collected in an inventory, so it is helpful to establish relationships linking tree height, crown length, crown radius, and DBH. We obtained data from several sources to do this. The Quebec data set included measurements on 534 trees from 24 mixed-species, clay soil sites within 80 km of Lac Duparquet. Every tree had measurements of DBH, height, crown length, and crown radius in four cardinal directions taken with a clinometer and measuring tape during 1999 (P. Bartemucci, personal communication). In Alberta, we used our 68 on-site ground survey trees (see previous section) to obtain similar data on DBH, height, and crown dimensions. We also obtained Alberta permanent sample plot data (Alberta Sustainable Resource Development 2002) for 4785 additional trees with crown length and DBH measurements, and temporary sample plot data (T. Vinge, Canadian Forest Products Ltd., personal communication) for 4133 additional trees with crown radius and DBH measurements. For height versus DBH functions, we used region-specific equations developed from measurements on 3510 felled trees by Huang et al. (1994). The range of these variables and sample size by species are shown in Table 2.

We examined linear and nonlinear equations in light of the physical and biological relationships that should exist between the dimensions and selected an equation for each relationship that had minimal and homogeneous residual variation. These were (eqs. 1–4)

[1] $H = 1.3 + a \times [1 - \exp(-b \times \mathrm{DBH})]^c$

[2] $L = a + b \times \mathrm{DBH} + c \times \mathrm{DBH}^2$

[3] $R = a + b \times \mathrm{DBH} + c \times \mathrm{DBH}^2$

[4] $L = b \times H + c \times R$

where H is tree height, L is crown length, R is crown radius, and a, b, and c are coefficients specific to each equation and species. We chose eq. 1 (a Chapman-Richards function) because the exponent c allowed for more flexibility and better fit than the two-parameter curves frequently used in mensuration (Huang et al. 1994; Husch et al. 2003). For the linear functions (eqs. 2–4), we sequentially removed intercept, linear, or quadratic terms that were not significant, and examined residuals for evidence of more complex relationships. Intercepts for eqs. 2–3 were restricted to prevent unreasonable values: intercepts a that were initially estimated at values

Table 2. Coefficients and statistics for equations used to predict crown dimensions.

Species	Lac Duparquet, Quebec[†]							Calling Lake, Alberta						
	a	b	c	n	Mean (min–max)	RMSE	R^2	a	b	c	n	Mean (min–max)	RMSE	R^2
Height (H), $H = 1.3 + a \times (1 - \exp[-b \times DBH])^c$														
Aspen	25.05	0.089	1.63	86	18.9 (5.5–30.8)	2.71	0.84	24.84	0.0808	1.241	1836‡	18.9 (2.2–31.9)	0.49	0.91
Balsam poplar								25.38	0.0501	0.927	236‡	17.8 (2.9–32.0)	0.53	0.87
Paper birch	18.00	0.162	2.24	68	14.4 (5.1–27.2)	2.92	0.68	27.97	0.0352	0.870	101‡	11.9 (3.2–21.5)	0.57	0.86
White spruce	25.19	0.082	2.19	63	18.4 (3.3–28.3)	2.69	0.82	29.88	0.0556	1.391	1176‡	20.3 (1.7–38.4)	0.58	0.90
Black spruce	19.17	0.128	2.27	59	13.9 (4.3–22.6)	1.84	0.85					12.2 (1.8–30.6)		
Balsam fir	26.60	0.054	1.22	71	14.1 (5.9–23.9)	2.02	0.85	28.63	0.0523	1.447	161‡	15.8 (1.8–31.4)	0.59	0.91
White cedar	18.52	0.036	0.86	88	11.7 (5.3–19.7)	1.64	0.81							
Jack pine	21.90	0.207	6.56	99	18.6 (4.6–27.5)	2.05	0.91							
Crown length (L), $L = a + b \times DBH + c \times DBH^2$														
Aspen	**1.30**	0.288	−0.0022	86	6.8 (1.9–13.9)	1.91	0.44	**1.30**	0.285	−0.0028	3595§	6.0 (0.3–28.0)	2.03	0.30
Balsam poplar								**1.30**	0.310	−0.0021	667§	7.5 (0.7–20.7)	2.40	0.48
Paper birch	1.17	0.423	−0.0046	68	6.5 (2.1–17.2)	2.14	0.54	0.92	0.315		179§	5.9 (0.8–19.2)	1.78	0.34
White spruce	**0.00**	0.598	−0.0045	63	11.8 (0–24.5)	2.25	0.78	**1.30**	0.437	−0.0012	25§	12.7 (0.4–34.3)	2.66	0.52
Black spruce	**0.00**	0.668	−0.0080	59	8.2 (1.8–16.1)	2.02	0.66							
Balsam fir	0.80	0.516	−0.0014	71	8.7 (2.5–19.9)	2.21	0.73	0.53	0.522		319§	8.8 (0.6–25.3)	2.46	0.56
White cedar	**1.30**	0.325	−0.0023	88	7.1 (1.9–15.5)	1.83	0.65							
Jack pine	**1.30**	0.254	−0.0009	99	6.6 (2.9–15.9)	1.64	0.56							
Crown radius (R), $R = a + b \times DBH + c \times DBH^2$														
Aspen	0.56	0.056		86	2.0 (0.2–4.9)	0.51	0.75	0.03	0.109	−0.0009	1581¶	20.5 (9.0–33.8)	0.49	0.48
Balsam poplar								0.60	0.062		64¶	18.7 (9.0–28.5)	0.46	0.57
Paper birch	0.67	0.059		68	1.7 (0.6–4.7)	0.42	0.68	**0.00**	0.083		14¶	18.2 (7.3–21.0)	0.44	0.51
White spruce	0.59	0.035		63	1.5 (0.5–3.4)	0.45	0.46	0.47	0.047		2343¶	18.7 (3.5–33.7)	0.46	0.45
Black spruce	0.59	0.031		59	1.1 (0.4–1.8)	0.26	0.37							
Balsam fir	0.72	0.036		71	1.3 (0.4–2.4)	0.36	0.37	0.34	0.054		131¶	17.5 (6.4–27.5)	0.44	0.46
White cedar	0.68	0.039		88	1.5 (0.5–3.1)	0.36	0.62							
Crown length (L), $L = b \times H + c \times R$														
Aspen		0.214	1.29	86	6.8 (1.9–13.9)	1.89	0.56		0.167	1.78	44#	7.0 (3.1–13.5)	1.36	0.61
Balsam poplar														
Paper birch		0.381	0.66	68	6.5 (2.1–17.2)	1.95	0.60							
White spruce		0.493	1.96	63	11.8 (0–24.5)	2.03	0.84		0.172	1.82	25#	8.9 (3.8–16.0)	2.36	0.64
Black spruce		0.473	1.60	59	8.2 (1.8–16.1)	1.95	0.70							
Balsam fir		0.472	1.79	71	8.7 (2.5–19.9)	1.85	0.84							
White cedar		0.566	1.33	88	7.1 (1.9–15.5)	1.48	0.79							
Jack pine		0.459	1.23	99	6.6 (2.9–15.9)	1.55	0.61							

Notes: Parameters shown in bold were fixed at zero or breast height (1.30 m) to prevent out-of-range (negative crown length or radius, crown length > height) values. Other parameters are significantly greater than zero at $\alpha = 0.05$. RMSE, root mean square error. DBH, diameter at breast height.

*DBH in centimetres; all other dimensions in metres.

†All Quebec crown data collected in 24 plots in the Lac Duparquet region.

‡Alberta height versus DBH coefficients and statistics from Huang et al. (1994).

§Alberta crown length and DBH data from the Alberta Land and Forest Division permanent sample plot program (Alberta Sustainable Resource Development 2002).

¶Alberta crown radius and DBH data from temporary sample plots in northern Alberta (T. Vinge, personal communication).

#Alberta crown length, height, and crown radius data collected at the Calling Lake site (see Materials and methods).

less than zero were subsequently fixed at zero. Likewise, for crown length, an intercept that exceeded 1.3 m was fixed at 1.3, since crown length at zero DBH cannot exceed breast height. Fixed intercept values are shown in bold in Table 2.

For developing the crown map at Lac Duparquet, our measured data consisted of mapped stem positions, a species identification, and tree DBH. We used eqs. 1–3 to estimate tree height, crown length, and radius. At Calling Lake, we had aerial photo-determined tree locations, species, height, and crown radius measurements, but required DBH and crown length data. We inverted eq. 1 to estimate DBH from photo-measured height and used eq. 4 to predict crown length from photo-measured height and crown radius.

PAR measurements

For PAR measurements, we constructed sensors, employing gallium arsenide phosphide photocells (G-2711-01, Hamamatsu Ltd., Bridgewater, New Jersey), following Fielder and Comeau (2000). The sensors used for daily PAR measurement were attached to inexpensive millivolt-precision dataloggers (Model H08-006-04, Onset Computer Corp., Pocasset, Massachussetts) and measured the current leakage of a 3-V power supply (two AA batteries) across the photocell in response to illumination (Stadt 2002). Sensors used for seasonal measurements were attached to microvolt-precision dataloggers (Model CR10X, Campbell Scientific, Edmonton, Alberta) and measured the current produced by the photocell because of illumination (Fielder and Comeau 2000). The sensor–datalogger combinations were checked against a commercial PAR sensor (LICOR 190SA, LICOR, Lincoln, NB) attached to a CR10X microvolt datalogger for 48 h on a rooftop before and after each growing season. Correlation between our sensors and the commercial one was satisfactory, even at very low PAR ($r \geq 0.98$ for 0–1600 $\mu mol \cdot m^{-2} \cdot s^{-1}$, $r \geq 0.95$ for 0–100 $\mu mol \cdot m^{-2} \cdot s^{-1}$). Two sensors failed in the 2000 season as a result of corrosion due to a poor diffuser seal.

For the inside canopy measurements at the two sites, sensors were placed at 34–36 microsites, at least 25 m from any edge of the mapped region. At Lac Duparquet, 20 of the sensors were placed beneath the mountain maple shrub layer, while the other 16 were positioned above. Sensor positions were mapped by horizontal distance, bearing, and elevation difference from the nearest survey stake. The sensors were left to sample and record PAR every 20 s for one day with mixed sunny and cloudy weather (27 July 1999, 0900–1700 h EDT at Lac Duparquet; 24 August 2000, 0900–1800 h MDT at Calling Lake). In addition, five additional sensors at Calling Lake were sampled once per minute, and the average stored every hour by a precision datalogger (CR10X, Campbell Scientific, Edmonton, Alberta) for two months (27 June – 22 July and 28 August – 15 September 2000). These provided a seasonal estimate of the PAR at these microsites.

For the above-canopy PAR estimate (P_t), another sensor was attached to a CR10X microvolt-precision datalogger and placed approximately 500 m away in a clearing with a nearly complete hemispherical sky view. A shadow-grid sensor, which measures direct (P_D) and total (P_t) PAR (Model BF2, Delta-T Devices Ltd., Cambridge, UK), was also attached to this "outside" datalogger at the Calling Lake site. For most of the growing season, the outside datalogger sampled its sensors every minute and averaged and stored data every hour.

During days when the 34–36 inside-canopy microsites were being measured, sampling and storage frequency of PAR on the outside datalogger was increased to 20 s to match the frequency of these inside-canopy sensors. %PAR was calculated by averaging the PAR readings inside and outside the forest first, then dividing the inside average by the outside average to calculate the transmission fraction. This corresponds with the sequence that MIXLIGHT uses to calculate PAR transmission (see following section).

At many microsites at Lac Duparquet and some at Calling Lake, shrub vegetation also obscured the sensors' sky view. For these, we made visual estimates of the total vertically projected percent vegetation cover (the percent ground area obscured by plants) to calculate the effect of this vegetation on %PAR (see following section).
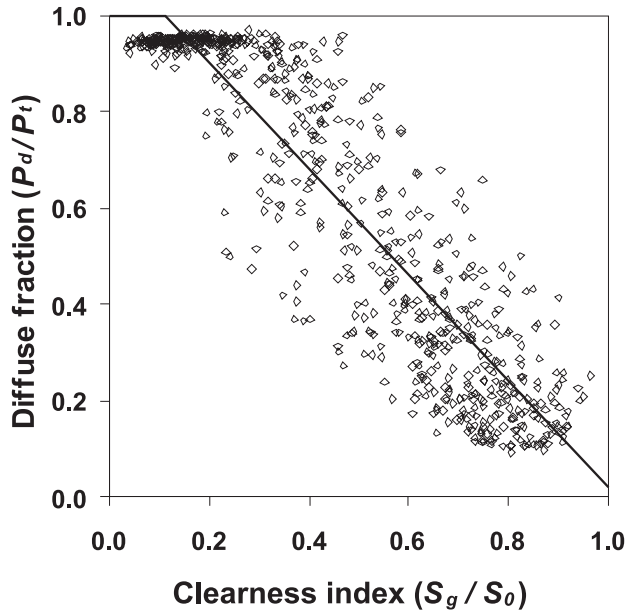
PAR transmission modeling

MIXLIGHT is a spatially explicit PAR transmission simulator designed for predicting %PAR levels in mixed-species boreal forests (Stadt and Lieffers 2000). MIXLIGHT represents tree stems and crowns as three-dimensional volumes (cylinders, cones, paraboloids, ellipsoids, combinations), defined by their crown dimensions (height, length, and radius) and located at their mapped crown position, then calculates PAR transmission by the weighted average gap probability along numerous rays traced across the upper hemisphere (480 rays were used in this study). A hemispherical sky radiance distribution is generated by tracking the sun's position and using the measured or estimated fractions of direct and diffuse PAR for short intervals (e.g., hours or minutes) during the full simulation interval. Diffuse radiance is set to follow a standard overcast angular distribution (Steven and Unsworth 1980). This calculation of the sky angular distribution is modified from Canham (1988), and a similar approach is described in detail by Smolander and Stenberg (2001). Rays are traced from the sky hemisphere to the simulation location. Where a ray passes through a tree crown envelope, the transmission along the ray is calculated by the Poisson probability of encountering no leaves, given the crown's leaf area density (LAD), an ellipsoidal leaf inclination distribution (controlled by parameter χ) at the zenith angle (Z) of the ray ($G(Z; \chi)$, Campbell and Norman 1989), and the length of the ray through the crown (S) (eq. 5).

$$[5] \qquad T(\alpha, Z) = \exp[-G(Z; \chi)\ S\ LAD]$$

Rays that hit boles below the live crown have their transmission set to zero. Rays passing below the edge of the plot have PAR transmission calculated on a canopy level (i.e., treating the entire stand as one large volume, similar to Black et al. 1991), using eq. 5 and a whole-plot estimate of $G(Z; \chi)$, S, and LAD. The ray transmission values are weighted by the radiance of the part of the sky where they originated, then averaged to give the overall transmission value to this microsite.

LAD and inclination parameters were obtained from Stadt and Lieffers (2000). This earlier study showed remarkably constant LAD for mature boreal trees from site to site. No adjustments were made to these parameters in the simulations reported here. We did not have data on leaf area density for some of the species occurring in low numbers in the Lac Duparquet site (black spruce, white cedar, and jack pine).

Fig. 1. Hourly diffuse fraction (P_d/P_t) of total PAR at Calling Lake, Alberta, versus the clearness index (S_g/S_0) for 27 June – 28 July and 22 August – 15 September 2000. The solid line is eq. 7 from text: $P_d/P_t = 1$ for $S_g/S_0 < 0.11$, $P_d/P_t = 1.12$–1.10 for $S_g/S_0 \geq 0.11$ ($n = 738$, RMSE = 0.13, $p < 0.001$, $R^2 = 0.84$).

Table 3. Leaf area density, leaf inclination, and crown shape parameters for tree species used in this study.

Species	Leaf area density ($m^2 \cdot m^{-3}$)	Ellipsoidal leaf inclination parameter (χ)	Crown shape
Aspen	0.44	0.82	Ellipsoid
Balsam poplar	0.30	1	Ellipsoid
Paper birch	0.80	1	Ellipsoid
White spruce	1.88	0.10	Rocket
Black spruce	2.00	0.10	Rocket
Balsam fir	1.98	1	Paraboloid
White cedar	1.80	1	Paraboloid
Jack pine	1.39	1	Ellipsoid

Note: Data from Stadt and Lieffers (2000), except for black spruce, white cedar, and jack pine, for which data were estimated by comparison with similar species (see Materials and methods).

estimate extraterrestrial irradiance (S_0) for each hour. The linear regression fit for eq. 7 is given in Fig. 1).

The input to MIXLIGHT consisted of the list of trees with their crown dimensions and positions, species-specific estimates of leaf area density and leaf inclination (Table 3), the site slope, aspect, latitude and longitude, the radiation data (local apparent time, total PAR, and diffuse fraction) during the simulation period, the microsite positions, and the vertically projected cover of understory vegetation above the microsite. The software output was an estimate of the PAR transmission to each microsite during the simulation period, as well as the percentage of the total sky radiance used to compute %PAR in the spatially explicit mode (rays traced above the plot edge). We simulated %PAR on a daily and seasonal basis and compared simulated values with measurements.

Since the overall objective of this work was to model tree growth as a function of seasonal %PAR available to each tree, the ideal test of the %PAR simulations should also be conducted on a seasonal basis. We could only commit five PAR sensors and one datalogger for one season at one site, so we also measured %PAR at numerous microsites, with a range of overlying canopy structures, over a full day where partial sun and cloud produced a complex above-canopy angular PAR distribution. Our assumption was that if MIXLIGHT could adequately simulate %PAR under this wide range of conditions for one day, then it should also perform adequately over the growing season (Gendron et al. 1998).

Tree growth measurements and analysis

At both sites, we selected understory saplings 0.2–7 m in height and without obvious leader damage, measured their total height (H) and the past three years' height growth, and plotted their location with reference to the nearest grid stake. Initial height was determined by subtracting the increments. The range of these values is reported in Table 4. Mean annual height growth was compared with initial height and MIXLIGHT's seasonal PAR transmission simulations for microsites located at the apices of the trees.

Additional data on growth versus height and %PAR for the region surrounding Lac Duparquet was provided by Y. Claveau. This data was from a study of factors controlling tree growth across the boreal forest (Claveau et al. 2002).

For these, we estimated leaf area density by visually comparing their crown density with similar species with known density.

PAR transmission through understory (shrub, herb) vegetation was modeled using a simple empirical equation, analogous to Beer's Law, but using visually estimated total vegetation cover above the microsite, rather than LAI, as the input variable (eq. 6). Derivation and testing of this equation is described in Stadt (2002).

$$[6] \qquad T = \left(1 - \frac{\% \, \text{cover}}{100}\right)^{0.52}$$

For the Lac Duparquet site, and in many anticipated uses of MIXLIGHT, only the total outside canopy PAR (P_t) was available. Both direct (P_D) and diffuse PAR (P_d) are necessary to develop the sky radiance distribution. We estimated the diffuse skylight fraction (P_d/P_t) from the clearness index (K = global irradiance / extraterrestrial irradiance at the time of measurement), following Roderick (1999) and Spitters et al. (1986). Equation 7 was fit to the hourly P_t and P_d (= P_t − P_D) measurements made with the shadow grid sensor over the 2000 growing season at Calling Lake:

$$[7] \qquad \begin{aligned} \frac{P_d}{P_t} &= 1 & \text{for } \frac{S_g}{S_0} < \frac{1-a}{b} \\ \frac{P_d}{P_t} &= a + b\,\frac{S_g}{S_0} & \text{for } \frac{S_g}{S_0} < \frac{1-a}{b} \end{aligned}$$

Global irradiance (S_g) was estimated by dividing the total PAR (P_t) reading by 2.04 µmol·J^{-1} (Meek et al. 1984), and the equations given by Spitters et al. (1986) were used to

Table 4. Characteristics (min–max) of understory saplings used to develop the predictive model for height growth.

	Lac Duparquet, Quebec	Lac Duparquet Region*	Calling Lake, Alberta
Species	Balsam fir	Balsam fir	White spruce
No. trees sampled	20	89	40
Initial height (m)	0.4–1.3	0.3–4.0	0.1–6.2
Mean annual height increment (cm/year)	1.8–28.8	0.2–35.0	1.5–38.3
%PAR	3–27[†]	1–78[‡]	1–52[†]

*Claveau et al. 2002.
[†]Simulated seasonal %PAR using MIXLIGHT.
[‡]PAR transmission on an overcast day.

Tree height, %PAR, and their interaction were identified as critical factors for balsam fir growth; however, no functional relationship was fit by these authors. Their study included 89 balsam fir saplings, 0.3–3.3 m tall, from three sites in the clay belt region surrounding Lac Duparquet. Sapling height and height increments over a 4-year period (1995–1998) were measured. PAR transmission was measured at the tree apex on overcast days using quantum sensors (LI190SA, LI-COR, Lincoln, Nebraska) or a plant canopy analyzer (LAI2000, LI-COR, Lincoln, Nebraska) (Gendron et al. 1998).

Michaelis-Menten and negative exponential functions were fitted to the sapling growth response to %PAR and initial height (Pacala et al. 1994). These functions saturate at a maximum value, as is the trend for growth increments over a wide range of initial heights and light levels (Lieffers and Stadt 1994; Pacala et al. 1994; Wright et al. 1998). Negative exponential functions provided the best fits and most easily interpretable parameters for both the initial height response and the seasonal PAR response. These were combined in eq. 8 to predict annual height growth (ΔH).

$$[8] \qquad \Delta H = \Delta H_{max}\left[1 - \exp\left(-\frac{H}{s_h}\right)\right]\left[1 - \exp\left(-\frac{\%PAR - a}{s_p}\right)\right]$$

where ΔH_{max} is the maximum height increment over an average growing season for tall saplings in full light; H is sapling height at the start of the year; a is a growth threshold for %PAR, since there may be no growth at low %PAR values; and s_h and s_p are scaling parameters for the height and seasonal PAR response, respectively (i.e., H and %PAR at 63% of ΔH_{max}).

Statistical analysis

Statistical analysis was performed using the correlation, linear, and nonlinear regression model procedures in SAS (Version 8e) (SAS Institute Inc. 2001). For nonlinear regression, the Gauss–Newton method was used. Significance was defined at the 5% level.

Results

PAR predictions

Average seasonal %PAR transmission simulated by MIXLIGHT at the Calling Lake site was well correlated with measured values at the five microsites that were monitored for 2 months in 2000 ($r = 0.93$, $p = 0.024$), and a plot

of predicted versus measured values approximated the 1:1 line (Fig. 2). Average daily simulated %PAR was also well correlated with measured daily values (Fig. 3; $r = 0.81$, $n = 36$, $p < 0.001$ for Lac Duparquet; $r = 0.76$, $n = 34$, $p < 0.001$ for Calling Lake). The relationship between simulated and measured values was very close to 1:1 for the Lac Duparquet site (Fig. 3a). At Calling Lake, however, MIXLIGHT tended to overestimate %PAR at the brighter microsites (Fig. 3b), which were located in a long, narrow gap.

Tree height growth

For the two balsam fir data sets from western Quebec (collected for this study and by Claveau et al. 2002), annual height growth (ΔH) increased with simulated seasonal %PAR, reaching its maximum at about 40% PAR (Fig. 4a). Height growth also increased with initial sapling height (H). Although the amount of increase in height increment declined with increasing height (curve was concave downward), no maximum was evident in these data (data not shown). Likewise, at Calling Lake, white spruce annual height growth increased with simulated seasonal PAR transmission values (Fig. 4b) and with tree height ($r = 0.55$, $n = 40$, $p < 0.001$). A concave downward trend was also evident, both with increasing %PAR and with initial height, but no maximum increment was evident.

Since taller trees may receive more light because of their higher canopy position, we examined correlation between initial height and %PAR. In the Calling Lake and Claveau et al. (2002) data sets, correlation between initial height and %PAR was not significant ($r = 0.23$, $p = 0.154$ and $r = 0.03$, $p = 0.760$, respectively). Initial height and %PAR were correlated in our Lac Duparquet data ($r = 0.89$, $p < 0.001$), but not when this was combined with the data from Claveau et al. (2002) to fit eq. 8 ($r = 0.09$, $p = 0.329$).

A saturating trend was suggested by scatter plots of growth versus initial height and %PAR (Fig. 4). However, unconstrained fits of eq. 8 yielded unreasonably large values of the maximum potential height increment (ΔH_{max}). None of the data sets contained points at sufficient height and high light to allow an accurate estimate this parameter. To constrain these values for predicting reasonable growth rates for tall trees in high light above the range of our data, we set ΔH_{max} to the maximum slope of the site index curve (SI, breast height age 50) for the same ecosite. Site index is determined from the 100 largest diameter trees/ha (Huang 1997), which are usually the tallest trees and those receiving the most light. For white spruce on BMe ecosites in the central mixed-

Fig. 2. Simulated seasonal versus measured PAR transmission from 27 June – 28 July and 22 August – 15 September 2000 (simulation runs over both periods) at five microsites at Calling Lake, Alberta (r = 0.93). The solid line shows the 1:1 relationship.
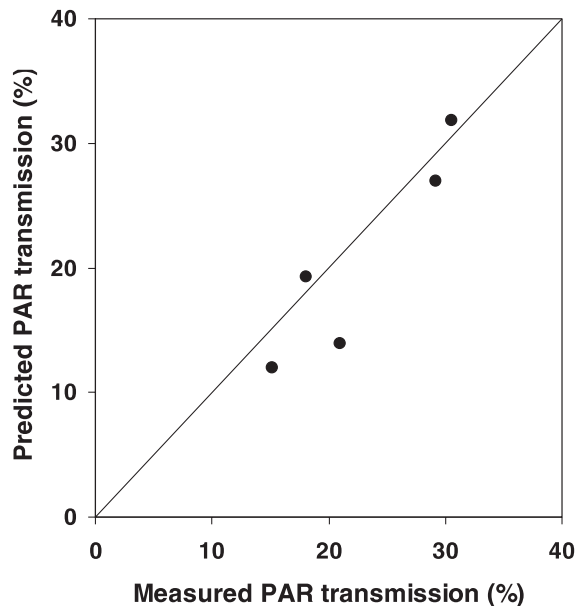
wood region of Alberta, SI = 17.8 m, which gives ΔH_{max} = 37.4 cm (Beckingham and Archibald 1996; Huang 1997). For balsam fir, ΔH_{max} = 38 cm for SI = 17 m on MS23 ecosites (Grondin et al. 2000). This method of choosing ΔH_{max} is sensitive to the site index, ΔH_{max} varying ±2 cm for SI ±1 m.

With ΔH_{max} fixed at these site index derived values, eq. 8 predicted annual height growth of balsam fir and white spruce effectively (Figs. 4 and 5). Fir survives at very low %PAR values, so the %PAR threshold (a, eq. 8) was not significant and was therefore removed from the model. For spruce, no saplings were found at very low %PAR, consequently a was significantly greater than zero. Some underestimation was evident at high growth rates (Fig. 5). This may be the result of increased allocation of resources to height growth for trees growing in the understory compared with the open-grown site index trees from which ΔH_{max} was derived (Duchesneau et al. 2001).

Discussion

%PAR modeling

MIXLIGHT was able to model the spatial variation in PAR transmission at the microsite level across two highly heterogeneous mixed-species boreal stands, one in eastern Canada and one in the west. Close correspondence between simulated and measured seasonal PAR was demonstrated in microsites monitored for most of the growing season, and similar values were obtained for full-day %PAR at both sites. This correspondence was valid for microsites with PAR transmission values from 1% to 45%. These results illustrate that the models used in MIXLIGHT for above-canopy radiation, overstory, and understory light penetration were effective for PAR prediction at daily and seasonal intervals.

The accuracy and precision of the MIXLIGHT simulator is similar to that reported for other spatially explicit radiation simulators that have been tested in forests (Canham et al. 1994, 1999; Cescatti 1997; Brunner 1998; Comeau et al. 1998; Groot 2004). However, we compared the daily or seasonal predictions of MIXLIGHT against direct PAR measurements rather than estimates of PAR derived from hemispherical photo analysis. Hemispherical photo predictions are generally well correlated with PAR, but are subject to considerable operator subjectivity (Wagner 1998) and are not effective for low-light microsites (Gendron et al. 1998; Machado and Reich 1999).

Like Norman and Welles (1983), Cescatti (1997), and Brunner (1998), MIXLIGHT uses the leaf area contained within an individual tree crown envelope for determining PAR transmission. The flexible leaf area envelope approach contrasts with SORTIE (Canham et al. 1994, 1999), where the crowns are represented as rectangular screens with a fixed transmission factor independent of the light angle (cf. eq. 5). There may be few differences among these models for predicting forest floor light levels, but the choice of crown shape becomes important for modeling the light profile with height. The leaf area approach also allows compatibility with coarser-scale models (e.g., Black et al. 1991) designed for simulating energy and mass transfer.

A number of problems make the development, application, and testing of a spatial PAR transmission model difficult. Crown representation is a major challenge. Geometric shapes chosen for the crown envelope seldom capture the full range of actual crown profiles. Highly flexible superellipsoids are quite effective (Cescatti 1997; Groot 2004), but obtaining measurements to fit unique shapes to each tree is currently time consuming. We anticipate the development of very fine resolution remote sensing techniques (Brandtberg et al. 2003; Omasa et al. 2003), which may allow recognition and precise characterization of individual tree crowns. Use of flexible crowns in a dynamic growth model also requires rules for controlling crown shape as the trees grow. The fixed geometric crown shapes used here (ellipsoids, paraboloids, cones, cylinders) with circular cross-sections had dimensions (length, width) that could be easily obtained or predicted from aerial-photo or ground-determined DBH or height, yet were adequate to model the daily and seasonal PAR attenuation by the trees.

Relatively strong relationships exist between stem diameter and tree height, but the relationships among crown dimensions (length, width) are more variable (Table 2). These dimensions are also controlled by PAR availability (Duchesneau et al. 2001; Claveau et al. 2002) and light quality (Gilbert et al. 2001), hydraulic constraints (Protz et al. 2000), abrasion from neighbour crowns (Rudnicki et al. 2003), winter temperatures (Lieffers et al. 2001), snow loading (King 1997), and likely site quality and moisture availability. Some work has recommended the use of both height and DBH to estimate crown dimensions (Pretzsch et al. 2002; Rudnicki et al. 2003). However, with the relatively small, complete data sets available (only 68 trees had all tree and crown dimensions measured in Alberta and 534 in Quebec), we were not able to improve on our simple functions of DBH or height alone (data not shown). Some improvement may be obtained by altering the crown length function for gap edges, since gap-

Fig. 3. Simulated versus measured daily PAR transmission. (*a*) Lac Duparquet, Quebec, 27 July 1999, *n* = 36 microsites, *r* = 0.81. (*b*) Calling Lake, Alberta, 24 August 2000, *n* = 34, *r* = 0.76. Solid lines show the 1:1 relationship.
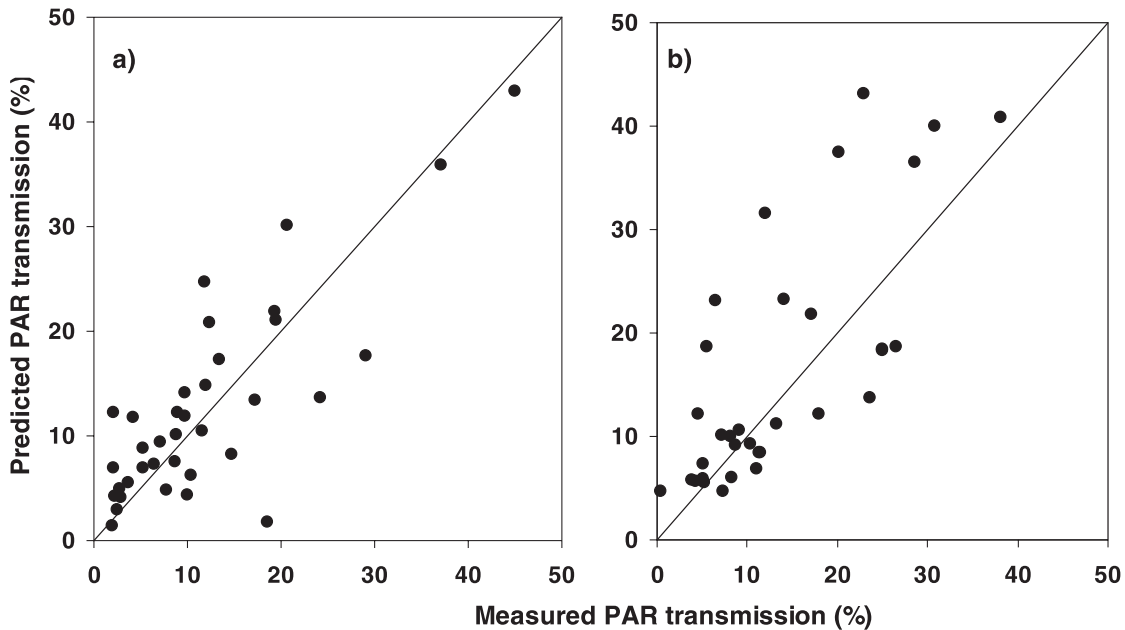

Fig. 4. Measured and predicted annual height growth (eq. 8, cm/year) as a function of seasonal %PAR and sapling height (m). (*a*) Balsam fir in western Quebec; symbols show measured values by height class: small ▲■: $H \leq 0.75$ m; small △□: $0.75 > H \leq 1.5$ m; large ▲■: $1.5 > H \leq 3$ m; large △□: $H > 3$ m. Triangles represent data collected in the present study, squares represent data from Claveau et al. (2002); solid lines show the fitted growth response (eq. 8) to %PAR at the initial heights shown: $\Delta H = 38.0[1 - \exp(-H/1.38)][1 - \exp(-\%PAR/12.8)]$, ($R^2 = 0.77$, $n = 109$, RMSE = 3.79, $p < 0.001$). (*b*) White spruce in central Alberta, symbols show measured values by height class: small ▲: $H \leq 0.75$ m; small △: $0.75 > H \leq 1.5$ m; large ▲: $1.5 > H \leq 3$ m; large △: $H > 3$ m. Solid lines show the fitted growth response to %PAR at the initial heights shown: $\Delta H = 37.4 [1 - \exp(-H/1.11)]\{1 - \exp[-(\%PAR - 4.41)/23.0]\}$, ($R^2 = 0.75$, $n = 40$, RMSE = 5.27, $p < 0.001$). Note that the values predicted by this function above 45% PAR are primarily driven by the ΔH_{max} value derived from the site index curve. Extrapolation into this region should be done with caution.
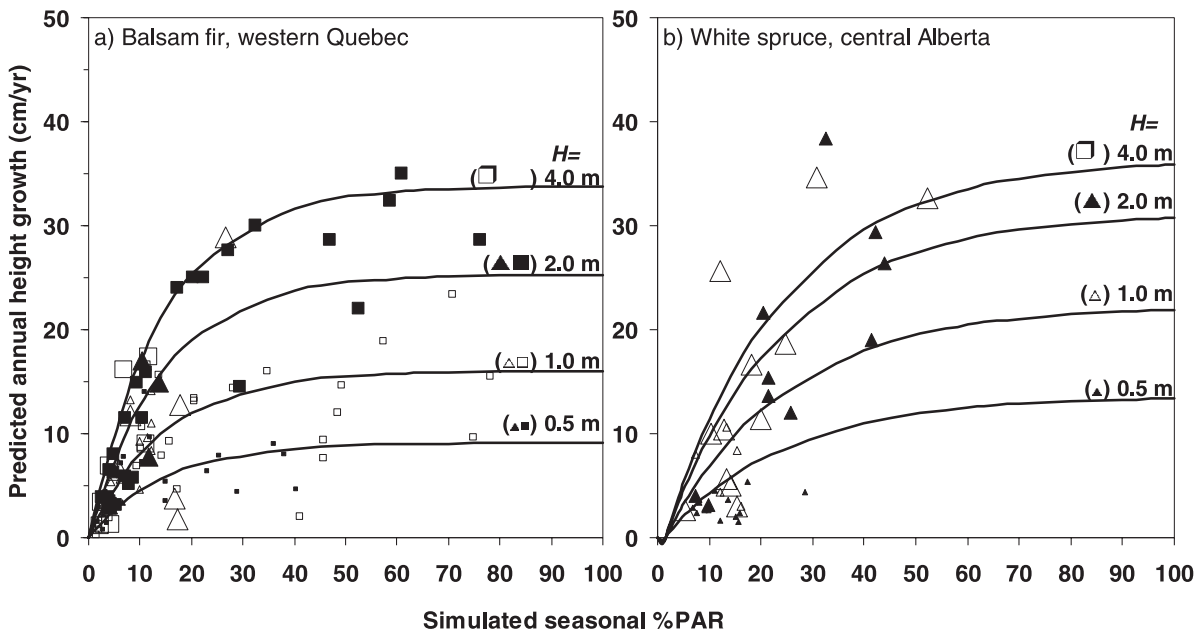
edge trees typically maintain longer crowns than interior trees. Our failure to compensate for gap-edge crown dimensions was likely the cause of overestimated daily light regimes within a large gap at Calling Lake.

Another issue is the occurrence of leaning trees. Conifers are strongly gravitropic, but northern deciduous species demonstrate a propensity to lean into any adjacent gap. Mapped stem positions may be less meaningful than mapped crown

Fig. 5. Predicted versus measured annual height growth (ΔH, cm/year). (*a*) Balsam fir saplings in western Quebec: large (▲, △): ΔH predicted using eq. 8 (parameters in Fig. 4); closed symbols are data collected at Lac Duparquet, with %PAR simulated by MIXLIGHT; open symbols are data from Claveau et al. (2002), collected in the region surrounding Lac Duparquet, with %PAR measured on overcast days. (*b*) White spruce saplings in central Alberta: large (▲): ΔH predicted using eq. 8 (parameters in Fig. 4), from data collected at Calling Lake, with %PAR simulated by MIXLIGHT; small (□): ΔH predicted using the equation developed by Lieffers and Stadt (1994) in central Alberta; (×): ΔH predicted using the equation developed by Wright et al. 1998 in sub-boreal British Columbia. Solid lines show the 1:1 relationship.
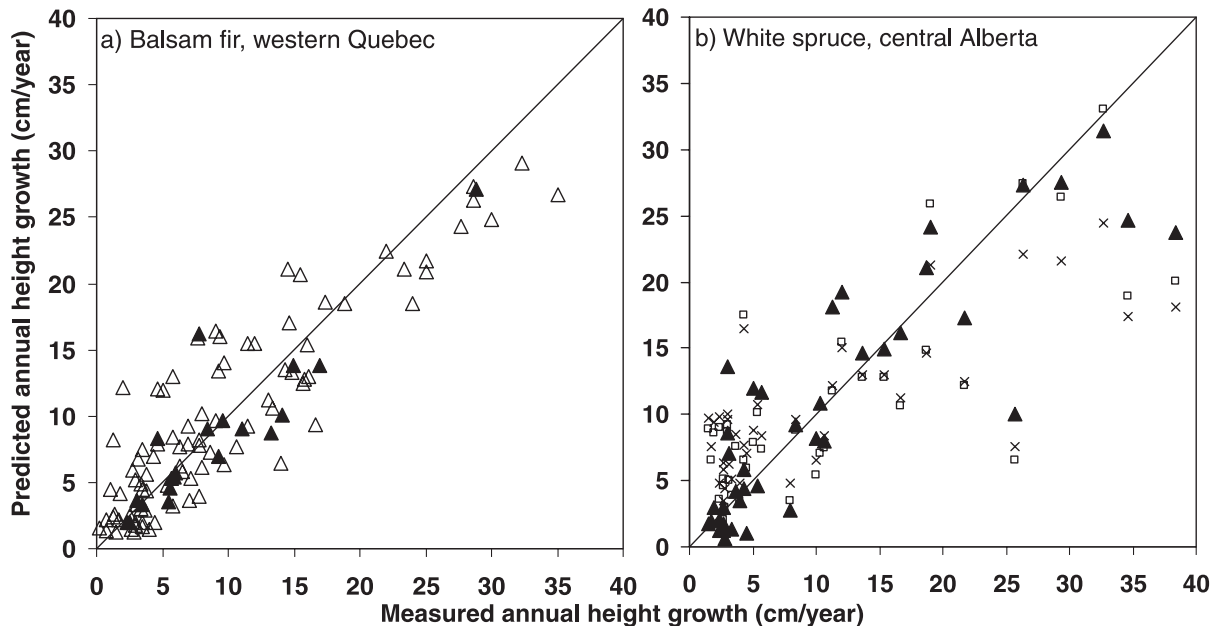
positions. For this reason, the aerial photo techniques used to map the Calling Lake site are preferable to the ground-based stem map used at Lac Duparquet.

The assumption of random leaf area within each crown envelope has been disputed. Canham et al. (1994) suggested the shade-tolerant species may approach a random distribution since foliage can persist deep within the crown, but that shade-intolerant species bear foliage primarily at the crown perimeter. If this is true, intolerant species may be better modeled as a screen of foliage rather than a volume (Canham et al. 1994; Groot 2004). However, the distribution of wood area should also be considered, as branch area is larger in the centre of a crown than at the periphery (Stadt and Lieffers 2000).

Lastly, an important practical problem in testing a %PAR model is that the "outside" canopy sensors must frequently be located some distance away from the "inside" sensors. Clouds frequently shade one but not the other set, creating uncontrolled variability in the transmission measurements.

Integration of PAR measurements over time tends to address most of these problems. The longer the integration interval, the more likely cloud shadows will affect inside and outside sensors equally. The sun traverses more of the sky and is more likely to be occluded by clouds, resulting in a radiance distribution that is less skewed toward one direction. Consequently, the shading effect of more neighbouring trees around each microsite is considered, which tends to even out variability in crown size and position. For these reasons, simulations will generally become more precise as the integration interval increases (cf. Figs. 2, 3*b*).

A potential source of bias in this %PAR model is the effect of site quality on stand and tree leaf area. With only two

sites measured in this study, it was not possible to examine the effects of moisture or nutrient regime on tree or stand leaf area density (LAD). Stadt and Lieffers (2000) estimated the average LAD for each species using optical techniques, but this study did not sample across the full range of ecosites. It is interesting to note that MIXLIGHT worked well in both of this study's sites, using the same species-specific LAD values, despite the eastern site receiving twice the precipitation as the west. Better sites may be able to support more leaf area index by maintaining larger crowns or a higher tree density. Nevertheless, the particular mechanisms of site effects on canopy light transmission have yet to be elucidated.

Growth modeling

PAR was a limited resource for the predominant understory species in these mixed-species boreal forests (balsam fir at Lac Duparquet and white spruce at Calling Lake), as shown by the positive response of height growth with PAR transmission. Height growth also increased with initial sapling height, but correlation between height and %PAR in the combined data sets was not significant. Since crown size increases with tree height in young trees, this suggests that crown absorption of PAR (APAR) controls height growth for balsam fir and white spruce.

Using a simulation model to calculate APAR in pure stands (Brunner 1998), MacFarlane et al. (2002) found little response in height growth to APAR for shade-intolerant loblolly pine, while Brunner and Nigh (2000) found a moderate response of mid-tolerant Douglas-fir. Wright et al. (1998) and Claveau et al. (2002) also found stronger responses of height increment to %PAR available for tolerant compared with intoler-

ant species. In a review of strategies of shade-tolerant and shade-intolerant species, Messier et al. (1999) illustrate that since intolerant species are adapted to early colonization after larger-scale disturbances, height growth usually improves their PAR capture. These species therefore inflexibly allocate carbon to height growth even under shaded conditions. By contrast, shade-tolerant species are adapted to the understory, where additional height will not improve their access to light until they reach the upper canopy. These species allocate carbon to larger leaves, wider crowns, and roots to maximize their capture of limited resources. It is not surprising then that an effect of %PAR on height growth is more evident in shade-tolerant species.

For white spruce, the height growth versus simulated %PAR relationship reported here is similar at lower %PAR levels to the height growth versus the clear-day, stand-average PAR transmission relationship reported in an earlier study (Lieffers and Stadt 1994), and the height growth versus hemispherical photo-estimated %PAR relationship developed by Wright et al. (1998) in British Columbia (Fig. 5*b*). However, both of those studies found lower maximum growth at high light levels. This may be a consequence of the different methods used to estimate %PAR, or because initial height was not accounted for in these studies. It is also possible that differences in site index between the sites used in these studies account for the differences in growth.

Conclusions

The effectiveness of a three-dimensional PAR simulator, MIXLIGHT, was demonstrated for daily and seasonal PAR transmission in 75 microsites at two mapped forest stands in the eastern and western Canadian boreal forest. Simulated transmission was also found to be effective for predicting the height growth of understory trees in these stands. The results suggest a PAR-driven process model of regeneration would work well in these forests and provide the flexibility to simulate early tree growth under mixed-species and partial-cut management systems.

Acknowledgements

References

Alberta Sustainable Resource Development. 2002. Permanent sample plot field procedures manual. Land and Forest Division, Forest Management Branch, Edmonton, Alta.

Bartelink, H.H. 2000. A growth model for mixed forest stands. For. Ecol. Manage. **134**: 29–43.

Beckingham, J.D., and Archibald, J.H. 1996. Field guide to ecosites of northern Alberta. Can. For. Serv. North. For. Cent. Spec. Rep. 5.

Black, T.A., Chen, J.M., Lee, X., and Sagar, R.M. 1991. Characteristics of shortwave and longwave irradiances under a Douglas-fir forest stand. Can. J. For. Res. **21**: 1020–1028.

Brandtberg, T., Warner, T.A., Landenberger, R.E., and McGraw, J.B. 2003. Detection and analysis of individual leaf-off tree crowns in small footprint, high sampling density lidar data from the eastern deciduous forest in North America. Remote Sens. Environ. **85**: 290–303.

Brunner, A. 1998. A light model for spatially explicit forest stand models. For. Ecol. Manage. **107**: 19–46.

Brunner, A., and Nigh, G. 2000. Light absorption and bole volume growth of individual Douglas-fir trees. Tree Physiol. **20**: 323–332.

Campbell, G.S., and Norman, J.M. 1989. The description and measurement of plant community structure. *In* Plant canopies: their growth, form, and function. *Edited by* G. Russell, B. Marshall, and P.G. Jarvis. Soc. Exp. Biol. Semin. Ser. **31**: 1–19.

Canham, C.D. 1988. An index for understory light levels in and around canopy gaps. Ecology, **69**: 1634–1638.

Canham, C.D., Coates, K.D., Bartemucci, P., and Quaglia, S. 1999. Measurement and modeling of spatially explicit variation in PAR transmission through interior cedar–hemlock forests of British Columbia. Can. J. For. Res. **29**: 1775–1783.

Canham, C.D., Finzi, A.C., Pacala, S.W., and Burbank, D.H. 1994. Causes and consequences of resource heterogeneity in forests: interspecific variation in PAR transmission by canopy trees. Can. J. For. Res. **24**: 337–349.

Cescatti, A. 1997. Modelling the radiative transfer in discontinuous canopies of asymmetric crowns. I. Model structure and algorithms. Ecol. Model. **101**: 263–274.

Claveau, Y., Messier, C., Comeau, P.G., and Coates, K.D. 2002. Growth and crown morphological responses of boreal conifer seedlings and saplings with contrasting shade tolerance to a gradient of light and height. Can. J. For. Res. **32**: 458–468.

Comeau, P., Macdonald, R. Bryce, R., and Groves, B. 1998. LITE: a model for estimating light interception through forest canopies, users manual and program documentation. B.C. Ministry of Forests, Research Branch, Victoria, B.C. Working Paper 35.

Duchesneau, R., Lesage, I., Messier, C., and Morin, H. 2001. Effects of PAR and intraspecific competition on growth and crown morphology of two size classes of understory balsam fir saplings. For. Ecol. Manage. **140**: 215–225.

Environment Canada. 2004. Canadian climate normals or averages 1971–2000 [online]. Available from http://www.climate.weatheroffice. ec.gc.ca/climate_normals/index_e.html [cited 9 May 2004].

Fielder, P., and Comeau, P. 2000. Construction and testing of an inexpensive PAR sensor. B.C. Ministry of Forests, Research Branch, Victoria, B.C. Working Paper 53/2000.

Gendron, F., Messier, C., and Comeau, P.G. 1998. Comparison of various methods for estimating the mean growing season percent photon flux density in forests. Agric. For. Meteorol. **92**: 55–70.

Gilbert, I.R., Jarvis, P.G., and Smith, H. 2001. Proximity signal and shade avoidance differences between early and late successional trees. Nature (Lond.), **411**: 792–795.

Grace, J.C., Jarvis, P.G., and Norman, J.M. 1987. Modelling the interception of solar radiant energy in intensively managed stands. N.Z. J. For. Sci. **17**: 193–209.

Grondin, P., Noël, J., Hotte, D., Tardif, P., and Lapointe, C. 2000. Croissance potentielle en hauteur et dynamique des espèces forestières sur les principaux types écologiques des régions écologiques 5*a* et 6*a* (Abitibi). Rapport Interne No. 461. Direction de

la recherche forestière, Ministère des Ressources naturelles, Gouvernement du Québec.

Groot, A. 2004. A model to estimate light interception by tree crowns, applied to black spruce. Can. J. For. Res. **34**: 788–799.

Huang, S. 1997. A subregion-based compatible height and site index model for young and mature white spruce in Alberta. Alberta Environmental Protection, Land and Forest Service, Edmonton, Alta. Publ. T/354; For. Manage. Res. Note 7.

Huang, S., Titus, S.J., Lakusta, S.J., and Held, R.J. 1994. Ecologically based individual tree volume estimation for major Alberta tree species. Report 2. Ecologically based individual tree height-diameter models for major Alberta tree species. Alberta Environmental Protection, Land and Forest Service, Forest Management Division, Edmonton, Alta.

Husch, B., Beers, T.W., and Kershaw, J.A., Jr. 2003. Forest mensuration. 4th ed. John Wiley and Sons, Hoboken, N.J.

King, D.A. 1997. Branch growth and biomass allocation in *Abies amabilis* saplings in contrasting light environments. Tree Physiol. **17**: 251–258.

Lieffers, S.M., Lieffers, V.J., Silins, U., and Bach, L. 2001. Effects of cold temperatures on breakage of lodgepole pine and white spruce twigs. Can. J. For. Res. **31**: 1650–1653.

Lieffers, V.J., and Stadt, K.J. 1994. Growth of understory *Picea glauca*, *Calamagrostis canadensis*, and *Epilobium angustifolium* in relation to overstory PAR transmission. Can. J. For. Res. **24**: 1193–1198.

MacFarlane, D.W., Green, E.J., Brunner, A., and Burkhart, H.E. 2002. Predicting survival and growth rates for individual loblolly pine trees from light capture estimates. Can. J. For. Res. **32**: 1970–1983.

Machado, J.L., and Reich, P.B. 1999. Evaluation of several measures of canopy openness as predictors of photosynthetic photon flux density in deeply shaded conifer-dominated forest understory. Can. J. For. Res. **29**: 1438–1444.

Meek, D.W., Hatfield, J.L., Idso, S.B., and Reginato, R.J. 1984. A generalized relationship between photosynthetically active radiation and solar radiation. Agron. J. **76**: 939–945.

Messier, C., Doucet, R., Ruel, J.C., Claveau, Y., Kelly, C., and Lechowicz, M. 1999. Functional ecology of advance regeneration in relation to light in boreal forests. Can. J. For. Res. **29**: 812–823.

Monteith, J.L. 1972. Solar radiation and productivity in tropical ecosystems. J. Appl. Ecol. **9**: 747–766.

Myneni, R.B., and Impens, I. 1985. A procedural approach for studying the radiation regime of infinite and truncated foliage spaces. Part I. Theoretical considerations. Agric. For. Meteorol. **33**: 323–337.

Norman, J.M., and Welles, J.M. 1983. Radiative transfer in an array of canopies. Agron. J. **75**: 481–488.

Omasa, K., Qiu, G.Y., Watanuki, K., Yoshimi, K., and Akiyama, Y. 2003. Accurate estimation of forest carbon stocks by 3-D remote sensing of individual trees. Environ. Sci. Tech. **37**: 1198–1201.

Pacala, S.W., Canham, C.D., and Silander, J.A. 1993. Forest models defined by field measurements: I. The design of a northeastern forest simulator. Can. J. For. Res. **23**: 1980–1988.

Pacala, S.W., Canham, C.D., Silander, J.A., and Kobe, R.K. 1994. Sapling growth as a function of resources in a north temperate forest. Can. J. For. Res. **24**: 2172–2183.

Perttunen, J., Sievanen, R., and Nikinmaa, E. 1998. LIGNUM: a model combining the structure and the functioning of trees. Ecol. Model. **108**: 189–198.

Pierce, L.L., and Running, S.W. 1988. Rapid estimation of coniferous forest leaf area index using a portable integrating radiometer. Ecology, **69**: 1762–1767.

Pretzsch, H., Biber, P., and Ďurský, J. 2002. The single-tree based stand simulator SILVA: construction, application and evaluation. For. Ecol. Manage. **162**: 3–21

Protz, C., Silins, U., and Lieffers, V.J. 2000. Reduction in branch sapwood hydraulic permeability as a factor limiting survival of lower branches of lodgepole pine. Can. J. For. Res. **30**: 1088–1095.

Roderick, M.L. 1999. Estimating the diffuse component from daily and monthly measurements of global radiation. Agric. For. Meteorol. **95**: 169–185.

Rudnicki, M., Lieffers, V.J., and Silins, U. 2003. Stand structure governs the crown collisions of lodgepole pine. Can. J. For. Res. **33**: 1238–1244.

SAS Institute Inc. 2001. SAS (Version 8e) [computer program]. SAS Institute Inc., Cary, N.C.

Smolander, S., and Stenberg, P. 2001. A method for estimating light interception by a conifer shoot. Tree Physiol. **21**: 797–803.

Spencer, R.D., and Hall, R.J. 1988. Canadian large-scale aerial photographic systems (LSP). Photogramm. Eng. Remote Sens. **54**(4): 475–482

Spitters, C.J.T., Toussaint, H.A.J.M., and Goudriaan, J. 1986. Separating the diffuse and direct component of global radiation and its implications for modeling canopy photosynthesis. Part I. Components of incoming radiation. Agric. For. Meteorol. **38**: 217–229.

Stadt, K.J. 2002. Modeling light for regeneration planning in mixed-species boreal forests. Ph.D. thesis, University of Alberta, Edmonton, Alta.

Stadt, K.J., and Lieffers, V.J. 2000. MIXLIGHT: a flexible PAR transmission model for mixed-species forest stands. Agric. For. Meteorol. **102**: 235–252.

Stadt, K.J., Landhäusser, S.M., and Stewart, J.D. 1997. Comment: the effects of direct-beam light on overcast-day estimates of light availability. Can. J. For. Res. **27**: 272–274.

Steven, M.D., and Unsworth, M.H. 1980. The angular distribution and interception of diffuse solar radiation below overcast skies. Q. J. R. Meteorol. Soc. **106**: 57–61.

Wagner, S. 1998. Calibration of grey values of hemispherical photographs for image analysis. Agric. For. Meteorol. **90**: 103–117.

Wright. E.F., Coates, K.D., Canham, C.D., and Bartemucci, P. 1998. Species variability in growth response to PAR across a climatic in northwestern British Columbia. Can. J. For. Res. **28**: 871–886.